

Spin-orbit coupling in ferromagnetic Nickel

J. Bünemann¹, F. Gebhard¹, T. Ohm², S. Weiser², and W. Weber²

¹ *Fachbereich Physik and Material Sciences Center, Philipps-Universität Marburg, D-35032 Marburg, Germany*

² *Fachbereich Physik, Universität Dortmund, D-44221 Dortmund, Germany*

We use the Gutzwiller variational theory to investigate the electronic and the magnetic properties of fcc-Nickel. Our particular focus is on the effects of the spin-orbit coupling. Unlike standard relativistic band-structure theories, we reproduce the experimental magnetic moment direction and we explain the change of the Fermi-surface topology that occurs when the magnetic moment direction is rotated by an external magnetic field. The Fermi surface in our calculation deviates from early de-Haas-van-Alphen (dHvA) results. We attribute these discrepancies to an incorrect interpretation of the raw dHvA data.

PACS numbers: 71.20.Be, 71.27.+a, 75.50.Cc, 71.10.Fd

The limitations of density functional theory (DFT) when treating the electronic and magnetic properties of transition metals become evident most clearly in the case of Nickel. The DFT cannot reproduce gross features such as the width of the $3d$ -bands (4.5 eV versus 3.3 eV experimentally^{1,2,3}), nor important details such as the exchange splitting. The exchange splitting in the DFT is almost 0.7 eV and rather isotropic over the Fermi-surface, whereas, experimentally, it is found to be much smaller and strongly orbital dependent: $\Delta_{e_g} \approx 0.17$ eV and $\Delta_{t_{2g}} \approx 0.33$ eV. As a result, even the Fermi surface topologies do not match, because of the position of the $X_{2,\downarrow}$ energy: above E_F in DFT, yet below E_F experimentally; thus only one hole ellipsoid exists around the X point, versus two in DFT.^{4,5}

Even more limitations of DFT become evident when the effects of the spin-orbit coupling are considered. The magnetic anisotropy energy has the wrong sign for Nickel (and for Cobalt), while it has the correct sign for Iron, yet is too small by a factor of three.⁶ In Nickel, the easy axis is along [111] and approximately $3 \mu\text{eV}$ per atom are needed to rotate the magnetic moment axis into the [001] direction.^{7,8} Moreover, a detailed low-temperature study of the magnetic anisotropy constants K_1, K_2, K_3 by Gersdorf⁸ has revealed a change in the Fermi-surface topology when the magnetic-moment axis is rotated into the [001] direction: A small second hole ellipsoid appears around the $X(001)$ point, but not around the $X(100)$ and $X(010)$ points, now inequivalent to $X(001)$, because of the underlying tetragonal symmetry.

It is generally accepted that the discrepancies between the DFT and the experimental results are mainly caused by an insufficient treatment of the electronic correlation in an effective one-particle theory. In the past, all attempts to combine the DFT with more sophisticated correlated electron theories have only led to partial improvements of the results for Nickel; see, e.g., the GW approximation in Ref. 9.

In a recent work⁴ we were able to show that a generalized Gutzwiller theory provides a consistent picture of the quasi-particle band-structure of Nickel. Neglecting spin-orbit coupling, all basic problems of the DFT calculations on Nickel have been resolved. Our theory employed ap-

proximately 2^{10} variational parameters representing the occupancies of all atomic multi-electron states within an open $3d$ shell (see below).

In this letter we present results for the case when spin-orbit coupling is included. In order to cope with this complication, the Gutzwiller theory had to be extended¹⁰ to allow for rotations in the eigenvector space of the atomic atomic multi-electron states, resulting in many more variational parameters. Employing this generalization we obtain the correct magnetic anisotropy energy, and, more importantly, reproduce the change in the Fermi-surface topology found by Gersdorf.

To investigate transition metals we start from multi-band Hubbard models of the general form

$$\hat{H} = \sum_{i \neq j; \sigma, \sigma'} t_{i,j}^{\sigma, \sigma'} \hat{c}_{i,\sigma}^\dagger \hat{c}_{j,\sigma'} + \sum_i \hat{H}_{\text{loc},i} = \hat{H}_0 + \hat{H}_{\text{loc}} \quad (1)$$

Here, the first term describes the hopping of electrons between spin-orbital states σ, σ' on lattice sites i, j , respectively. The Hamiltonian

$$\hat{H}_{\text{loc},i} = \hat{H}_{C,i} + \hat{H}_{\text{cf},i} + \hat{H}_{\text{SO},i} \quad (2)$$

contains all local terms, i.e., the two-particle Coulomb interaction $\hat{H}_{C,i}$, the crystal field energies $\hat{H}_{\text{cf},i}$ and the spin-orbit coupling $\hat{H}_{\text{SO},i}$. In the case of Nickel, we work with a basis of $3d$, $4s$, and $4p$ orbitals.

We have determined the bare hopping-parameters in the one-particle Hamiltonian \hat{H}_0 and the crystal-field energies in \hat{H}_{cf} by means of a tight-binding fit to the paramagnetic DFT band structure.^{4,10} Due to the large band-width of the $4s$ and $4p$ bands, only the Coulomb-interaction within the $3d$ -shell is taken into account. The spherical approximation is used, i.e., we express the Coulomb interaction through the three Racah-parameters A , B , and C .¹¹ Note that cubic site symmetry would allow ten independent interaction parameters. In order to reproduce the experimental d -band width in our approach, we need a Racah-parameter $A \approx 9$ eV. The Racah-parameters B and C are assumed to be close to their atomic values¹¹, $B \approx 85$ meV and $C \approx 400$ meV, resulting in a value J of $J = 7B/2 + 7C/5 \approx 0.85$ eV. The

spin-orbit coupling parameter ζ in the spin-orbit Hamiltonian

$$\hat{H}_{\text{SO},i} = \sum_{\sigma\sigma'} \frac{\zeta}{2} \langle \sigma | \hat{l}_x \tilde{\sigma}_x + \hat{l}_y \tilde{\sigma}_y + \hat{l}_z \tilde{\sigma}_z | \sigma' \rangle \hat{c}_{i,\sigma}^\dagger \hat{c}_{i,\sigma'} \quad (3)$$

is chosen as $\zeta = 80\text{meV}$. Note that the Hamiltonian (3) only contains d -orbitals.

In the Gutzwiller theory, the following Ansatz for a variational wave-function^{10,13,14} is used to investigate the multi-band Hubbard model (1)

$$|\Psi_G\rangle = \hat{P}_G |\Psi_0\rangle = \prod_i \hat{P}_i |\Psi_0\rangle. \quad (4)$$

Here, $|\Psi_0\rangle$ is a normalized single-particle product state and the local Gutzwiller correlator is defined as

$$\hat{P}_i = \sum_{\Gamma,\Gamma'} \lambda_{\Gamma,\Gamma'}^{(i)} |\Gamma\rangle_{ii} \langle \Gamma'|. \quad (5)$$

The states $|\Gamma\rangle_i$ form some arbitrary basis of the atomic Hilbert-space and the (complex) numbers $\lambda_{\Gamma,\Gamma'}^{(i)}$ are variational parameters. For Nickel, we work with a correlation operator (5) in which the states $|\Gamma\rangle_i$ are the eigenstates of the atomic Hamiltonian $\hat{H}_{C,i}$. The non-diagonal elements of the variational parameter matrix $\lambda_{\Gamma,\Gamma'}$ are assumed to be finite only for states $|\Gamma\rangle$, $|\Gamma'\rangle$ which belong to the same atomic multiplet. This is consistent with the spherical approximation for the Coulomb-interaction. In the case of Nickel, it is sufficient to work with non-diagonal parameters $\lambda_{\Gamma,\Gamma'}$ in the d^7 , d^8 and d^9 shells.

The expectation value of the Hamiltonian (1) can be calculated analytically for the Gutzwiller wave function (4) in the limit of infinite spatial dimensions.¹⁴ We use the exact results in this limit as an approximation for our three-dimensional model system. The Gutzwiller energy functional can also be obtained in slave-boson mean-field theory.^{16,17} In infinite dimensions one finds

$$\langle \hat{H}_{\text{loc},i} \rangle_{\Psi_G} = \sum_{\Gamma_1 \dots \Gamma_4} \lambda_{\Gamma_2,\Gamma_1}^* \lambda_{\Gamma_3,\Gamma_4} E_{\Gamma_2,\Gamma_3}^{\text{loc}} m_{\Gamma_1,\Gamma_4}^0 \quad (6)$$

for the expectation value of the local Hamiltonian in (1), where

$$E_{\Gamma_2,\Gamma_3}^{\text{loc}} \equiv \langle \Gamma_2 | \hat{H}_{\text{loc},i} | \Gamma_3 \rangle, \quad (7)$$

$$m_{\Gamma_1,\Gamma_4}^0 \equiv \langle (|\Gamma_1\rangle \langle \Gamma_4|) \rangle_{\Psi_0}. \quad (8)$$

The local expectation value (8) is readily calculated by means of Wick's theorem. For the expectation value of a hopping operator in (1) one finds

$$\langle \hat{c}_{i,\sigma_1}^\dagger \hat{c}_{j,\sigma_2} \rangle_{\Psi_G} = \sum_{\sigma'_1, \sigma'_2} q_{\sigma'_1}^{\sigma'_2} \left(q_{\sigma'_2}^{\sigma'_1} \right)^* \langle \hat{c}_{i,\sigma_1}^\dagger \hat{c}_{j,\sigma_2} \rangle_{\Psi_0}. \quad (9)$$

The renormalization matrix $q_{\sigma}^{\sigma'}$ in (9) can be calculated most easily when an orbital basis is used which has a diagonal local density-matrix with respect to $|\Psi_0\rangle$,

$$C_{\sigma,\sigma'}^0 \equiv \langle \hat{c}_{i,\sigma}^\dagger \hat{c}_{i,\sigma'} \rangle_{\Psi_0} = \delta_{\sigma,\sigma'} n_{\sigma}^0. \quad (10)$$

If $C_{\sigma,\sigma'}^0$ is non-diagonal for a one-particle product state $|\Psi_0\rangle$ one can always transform the orbital basis in order to ensure that Eq. (10) holds. In the case of a diagonal local density-matrix (10), the renormalization matrix in (9) reads

$$q_{\sigma}^{\sigma'} = \frac{1}{n_{\sigma'}^0} \sum_{\Gamma_1 \dots \Gamma_4} \lambda_{\Gamma_2,\Gamma_1}^* \lambda_{\Gamma_3,\Gamma_4} \langle \Gamma_2 | \hat{c}_{\sigma}^\dagger | \Gamma_3 \rangle \times \langle (|\Gamma_1\rangle \langle \Gamma_4| \hat{c}_{\sigma'}) \rangle_{\Psi_0}, \quad (11)$$

where, again, the expectation value with respect to $|\Psi_0\rangle$ is calculated with Wick's theorem.

The variational ground-state energy must be minimized with respect to the variational parameters $\lambda_{\Gamma,\Gamma'}$ and the one-particle product wave-functions $|\Psi_0\rangle$. It has been found^{10,18} that the optimum state $|\Psi_0\rangle$ is the ground state of the effective one-particle Hamiltonian

$$\hat{H}_0^{\text{eff}} = \sum_{i \neq j; \sigma, \sigma'} \tilde{t}_{i,j}^{\sigma, \sigma'} \hat{c}_{i,\sigma}^\dagger \hat{c}_{j,\sigma'} + \sum_{i; \sigma, \sigma'} \eta_{\sigma, \sigma'} \hat{c}_{i,\sigma}^\dagger \hat{c}_{i,\sigma'}. \quad (12)$$

Here, we introduced the renormalized hopping matrix elements

$$\tilde{t}_{i,j}^{\sigma_1, \sigma_2} = \sum_{\sigma'_1, \sigma'_2} q_{\sigma'_1}^{\sigma_1} \left(q_{\sigma'_2}^{\sigma_2} \right)^* t_{i,j}^{\sigma'_1, \sigma'_2} \quad (13)$$

and the Lagrange-parameters $\eta_{\sigma, \sigma'}$ which are used to optimize the energy with respect to the local density matrix (10). Within a Landau Fermi-liquid approach one can further show^{10,18} that the eigenvalues $E_\gamma(k)$ of \hat{H}_0^{eff} are the quasi-particle excitation energies that can be compared, for example, to ARPES experiments. Most important for the quasi-particle band-structure are the Lagrange-parameters $\eta_{\sigma, \sigma'}^d$ for the d -orbitals. The two (diagonal) Lagrange parameters for the s and p orbitals are adjusted in order to fix the total d -electron number.¹⁹

The inclusion of spin-orbit coupling in the Gutzwiller theory complicates the numerical minimization significantly. Both the d -part of the local density-matrix (10) and of the hopping renormalization matrix (11) are no longer diagonal. The number n_{ie} of independent elements depends on the magnetic moment direction, we find $n_{ie} = 22$ for $\vec{\mu} || [111]$ and $n_{ie} = 18$ for $\vec{\mu} || [001]$. As a consequence of the reduced symmetry, we could work with up to n_{ie} independent d -shell Lagrange parameters $\eta_{\sigma, \sigma'}^d$ in order to minimize the total energy. Numerically, however, such a minimization would be quite costly since each variation of these parameters involves many momentum-space integrations. We therefore work with a simplified effective Hamiltonian \hat{H}_0^{eff} that contains effective parameters only for all physically relevant one-particle terms.

In cubic symmetry, there exist only four independent matrix elements of the local (d -electron) density-matrix. The trace of the matrix is fixed by the total d -electron number. The three remaining matrix elements are governed by parameters $\eta_{\sigma, \sigma'}^d$ which are given by the orbital-dependent exchange fields $\Delta_{t_{2g}}$, Δ_{e_g} and the effective crystal-field splitting $\epsilon_{\text{CF}}^{\text{eff}}$.

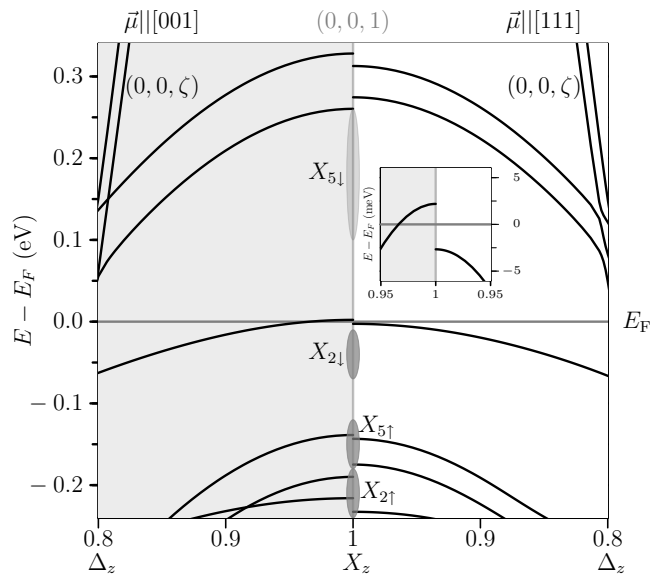


FIG. 1: Quasi-particle band structure along the Δ_z -line around the X_z -point of the Brillouin zone for magnetic-moment directions $\vec{\mu} \parallel [001]$ and $\vec{\mu} \parallel [111]$. The inset shows an enlarged view of the band structure around the Fermi energy which displays the additional hole ellipsoid for $\vec{\mu} \parallel [001]$ more clearly.

The non-cubic symmetry resulting from the addition of the spin-orbit coupling adds many more formally independent $\eta_{\sigma,\sigma'}^d$ terms. Both for $\vec{\mu} \parallel [001]$ (tetragonal symmetry) and for $\vec{\mu} \parallel [111]$ (trigonal symmetry) there are two more exchange-fields and two more crystal-field splittings. All these eight terms are included in our simplified effective Hamiltonian \hat{H}_0^{eff} . In the spirit of the spherical approximation¹², a Hamiltonian $\hat{H}_{\text{SO}}^{\text{eff}}$ is included in \hat{H}_0^{eff} that has the same form as \hat{H}_{SO} only with ζ replaced by ζ^{eff} . As a result, we have to minimize the total energy with respect to nine ‘external’ parameters in our simplified Hamiltonian \hat{H}_0^{eff} .

The numerical minimization is much more time-consuming for a system with spin-orbit coupling than without. First, spin-orbit coupling requires the momentum-space integration to be extended from 1/48th to the full Brillouin zone. Furthermore, the small values of the anisotropy energy necessitate a much finer mesh for the momentum-space integration. Second, the energy needs to be minimized with respect to nine external variational parameters in \hat{H}_0^{eff} . Altogether, the minimization of the total energy is approximately 10^4 times more time consuming for a system with spin-orbit coupling than in the absence of \hat{H}_{SO} .

We carried out the minimization of the variational energy with respect to the ‘internal’ parameters $\lambda_{\Gamma,\Gamma'}$ and the external parameters for both magnetic moment directions $\vec{\mu} \parallel [111]$ and $\vec{\mu} \parallel [001]$. The optimum value of the effective spin-orbit coupling is $\zeta_{\text{eff}} \approx 68$ meV in both cases, about 15% smaller than the bare value $\zeta = 80$ meV.

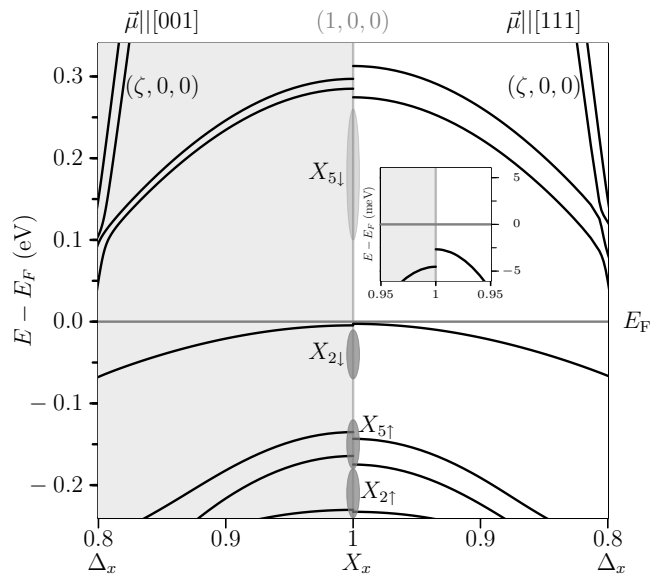


FIG. 2: Same as in Fig. 1 but around the X_x -point. Note that the $X_{2\downarrow}$ -band is below the Fermi energy for both magnetic-moment directions.

There seems to be no simple rule that determines the relative size of ζ and ζ_{eff} . For example, for Iron we found an effective spin-orbit considerably larger than the corresponding bare value. In our calculations for Nickel, the anisotropy energy is $E_{\text{aniso}} \approx 3.5 \mu\text{eV}$ per atom, quite close to the experimental value $E_{\text{exp}} \approx 3.0 \mu\text{eV}$. Note that this energy difference has to be calculated quite carefully within the Gutzwiller approach. In particular, one has to keep in mind that any approximation on the parameters $\lambda_{\Gamma,\Gamma'}$ that reduces the variational flexibility may lead to a grossly overestimated anisotropy energy. This is a serious problem, in particular, in the case of Iron. For Nickel, however, the active multiplet states belong mostly to d^8 and d^9 . Here, a mixing of states $|\Gamma\rangle, |\Gamma'\rangle$ has little effect on the variational energy, and even a diagonal variational parameter matrix $\lambda_{\Gamma,\Gamma'} \sim \delta_{\Gamma,\Gamma'}$ would lead to reasonable results.

In Figures 1 and 2 we show the quasi-particle band-structure that arises from our calculation around the X -points $X_z \equiv (001)$ and $X_x \equiv (100)$. When the magnetic moment is along the easy axis, the band-structure around both X -points coincides and the minority state $X_{2\downarrow}$ is below the Fermi-energy.²⁰ For a magnetic moment along the $[001]$ -direction, however, the two states $X_{2\downarrow}$ have different energies. The $X_{2\downarrow}$ state at X_x remains below the Fermi level, whereas the corresponding state at X_z creates a new hole pocket around this X -point. This is the scenario proposed by Gersdorf.⁸

In Figure 3 we show Fermi-surface cuts that we find within our Gutzwiller theory. The experimental values are taken from dHvA experiments by Tsui⁵ and by Stark as reported in Ref. 15. The agreement is quite satisfactory along high-symmetry lines, whereas there are significant discrepancies away from them. We do believe that

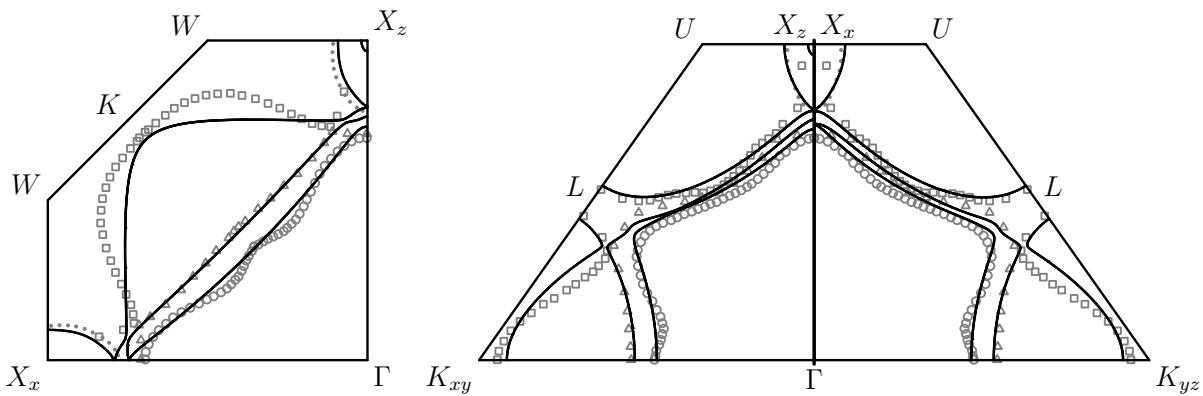


FIG. 3: Fermi-surface cuts with various planes in the Brillouin zone. Lines: Gutzwiller theory including spin-orbit coupling; Squares and triangles: experimental data reported in 15; Dots: experimental data of Tsui⁵.

the wiggles that appear in the experimental data are, in fact, spurious. The derivation of a Fermi surface from the raw dHvA data requires an expansion in Fermi surface harmonics, with the coefficients of the harmonics to be determined from least squares' fits to the data. Possibly, an over-determination occurred which led to unphysically large higher harmonics coefficients and resulted in the wiggles. We propose to redo these measurements.

In summary, we have resolved the long-standing problem to explain theoretically the electronic and magnetic properties of elementary fcc-Nickel. Our calculations are based on the Gutzwiller variational theory which is a powerful tool for the investigation of Fermi-liquid sys-

tems with medium to strong Coulomb interaction. For such systems, state of the art band-structure theories usually fail. Our results for the quasi-particle bands are in very good agreement with ARPES experiments and we find the experimental Fermi-surface topology. Furthermore, we are able to explain the subtle effects that the spin-orbit coupling has in Nickel. Our theory yields the correct anisotropy energy and we confirm the Gersdorf scenario: The Fermi-surface topology changes around the X -point (001) when the magnetic moment direction is rotated from $\vec{\mu}||[111]$ to $\vec{\mu}||[001]$ by an external magnetic field.

-
- ¹ D.E. Eastman, F.J. Himpsel, and J.A. Knapp, Phys. Rev. Lett. **40**, 1514 (1978).
² W. Eberhardt and E.W. Plummer, Phys. Rev. B **21**, 3245 (1980).
³ V.L. Moruzzi, J.F. Janak, and A.R. Williams, *Calculated Electronic Properties of Metals* (Pergamon Press, New York, 1978).
⁴ J. Bünemann, F. Gebhard, T. Ohm, R. Umstätter, S. Weiser, W. Weber, R. Claessen, D. Ehm, A. Harasawa, A. Kakizaki, A. Kimura, G. Nicolay, S. Shin, and V.N. Strocov, Europhys. Lett. **61**, 667 (2003).
⁵ D.C. Tsui, Phys. Rev. **164**, 669 (1967).
⁶ G.H.O. Daalderop, P.J. Kelly, and M.F.H. Schuurmans, Phys. Rev. B **41**, 11919 (1990).
⁷ R. Gersdorf and G. Aubert, Physica B **95**, 135 (1978).
⁸ R. Gersdorf, Phys. Rev. Lett. **40**, 344 (1978).
⁹ F. Aryasetiawan, Phys. Rev. B **46**, 13051 (1992).
¹⁰ J. Bünemann, F. Gebhard, and W. Weber, in *Frontiers in Magnetic Materials*, ed. by A. Narlikar (Berlin: Springer, 2005) p. 117; cond-mat/0503332.
¹¹ S. Sugano, Y. Tanabe, and H. Kamimura, *Multiplets of Transition-Metal Ions in Crystals* (Pure and Applied Physics **33**, Academic Press, New York, 1970).
¹² In cubic environment there should actually be two different parameters ζ in (3), one for the coupling amongst the t_{2g} orbitals and another one for the coupling between t_{2g} and

- e_g orbitals. Experimentally, however, no indication for such a correction has been found; J. Callaway and C. S. Wang, Phys. Rev. B **7**, 1096 (1973).
¹³ M.C. Gutzwiller, Phys. Rev. Lett. **10**, 159 (1963); Phys. Rev. **134**, A923 (1964); *ibid.* **137**, A1726 (1965).
¹⁴ J. Bünemann, W. Weber, and F. Gebhard, Phys. Rev. B **57**, 6896 (1998).
¹⁵ C.S. Wang and J. Callaway, Phys. Rev. B. **15**, 298 (1977); J. Callaway in *Physics of Transition Metals 1980*, ed. by P. Rhodes (Conf. Ser. Notes **55**, Inst. of Physics, Bristol, 1981), p. 1.
¹⁶ F. Lechermann, A. Georges, G. Kotliar, and O. Parcollet, Phys. Rev. B **76**, 155102 (2007).
¹⁷ J. Bünemann and F. Gebhard, Phys. Rev. B **76**, 193104 (2007).
¹⁸ J. Bünemann, F. Gebhard, and R. Thul, Phys. Rev. B **67**, 075103 (2003).
¹⁹ In the presence of spin-orbit coupling there may also be a finite parameter $\eta_{\sigma,\sigma'}$ for a coupling between the s -orbital and a certain d -state. However, we found that this term does not affect the results for Nickel significantly.
²⁰ Note that in the presence of spin-orbit coupling the spin label in X_{2d} is not well defined but merely refers to the main spin-component of this state.